Disorder-Induced Magnetoresistance in a Two-Dimensional Electron System

Jinglei Ping,[1,2,*] Indra Yudhistira,[3] Navneeth Ramakrishnan,[3] Sungjae Cho,[1,†] Shaffique Adam,[3,4,‡] and Michael S. Fuhrer[1,2,§]

[1]*Center for Nanophysics and Advanced Materials, University of Maryland, College Park, Maryland 20742-4111, USA*

[2]*School of Physics, Monash University, Victoria 3800, Australia*

[3]*Graphene Research Centre and Department of Physics, National University of Singapore, 2 Science Drive 3, 117551, Singapore*

[4]*Yale-NUS College, 6 College Avenue East, 138614, Singapore*

(Received 21 January 2014; published 25 July 2014)

We predict and demonstrate that a disorder-induced carrier density inhomogeneity causes magnetoresistance (MR) in a two-dimensional electron system. Our experiments on graphene show a quadratic MR persisting far from the charge neutrality point. Effective medium calculations show that for charged impurity disorder, the low-field MR is a universal function of the ratio of carrier density to fluctuations in carrier density, a power law when this ratio is large, in excellent agreement with experiment. The MR is generic and should occur in other materials with large carrier density inhomogeneity.

DOI: 10.1103/PhysRevLett.113.047206 PACS numbers: 75.47.−m

Introduction.—The classical magnetoresistance of a material arises when the Lorentz force caused by an applied magnetic field has a component acting against the direction of electron motion thereby decreasing the conductivity of an electronic material. This property has long been of interest both as a tool to probe the fundamental properties of an electronic material (such as the topology of the electron bands) [1] and also for technological applications such as its use in magnetic memory read-heads [2]. A well-known result is that single electronic bands (in systems with a spatially homogenous carrier density) will have no magnetoresistance, while the presence of two or more electronic bands with different carrier mobilities readily gives rise to a classical magnetoresistance [3]. This classical effect is different from weak localization [4] (a quantum interference effect present at low temperatures) or Abrikosov's quantum magnetoresistance [5] (that occurs in gapless semiconductors in the high field Landau quantized regime).

Graphene is an example of a material with more than one electronic band. This single-atom-thick sheet of carbon comprises an electron band and a hole band each with a linear dispersion that touch at a topologically protected Dirac point [6,7]. It was shown by Ref. [8] that if both bands are occupied, one then expects a classical magnetoresistance even if the electron and hole bands have the same electronic mobility (this is by virtue of the Lorentz force being of opposite sign for the electron and hole carriers). While this two-channel model has been reasonably successful at modeling the density dependence of graphene magnetotransport at fixed magnetic field, it is unable to quantitatively explain the magnetic field dependence at fixed carrier density. In this context, the authors of Refs. [9] and [10] developed an effective medium theory (EMT) approximation where the planar landscape is broken up into electron regions and hole regions with different area fractions but where each region had a uniform conductivity. This description fails to describe experiments away from the symmetry point (see Ref. [11] for a detailed discussion of these earlier theoretical and experimental results). However, we note that the two-channel model of Hwang *et al.* and the EMT calculation of Stroud and collaborators both predict that the magnetoresistance should vanish away from the Dirac point when only a single band is occupied. By contrast, in this work we discuss a carrier density inhomogeneity contribution to the magnetoresistance that persists away from the Dirac point and exists even if only one electronic band is occupied. For concreteness we focus our discussion on graphene which has a linear dispersion, but the mechanism itself does not rely on the linear dispersion and should therefore be observable in other materials with large spatial inhomogeneity in the carrier density distribution.

The idea of a disorder-induced magnetoresistance is not new. While working on silver chalcogenides, Parish and Littlewood [12,13] predicted such an effect by mapping the problem onto a random resistor network and solving it numerically. They focused only on the high magnetic field regime and found a linear magnetoresistance, but quantitative comparisons with experiments remained challenging [14]. By contrast, in this work, we develop a full effective medium theory to study the low field regime and make quantitative predictions that are then compared to experimental results. The basic mechanism for inhomogeneity-induced magnetoresistance is illustrated qualitatively in Fig. 1, where we show two regions with different local carrier densities. The Hall field, which only depends on the average carrier density, is the same in both regions and is perpendicular to both the applied electric field and the applied magnetic field. As seen in the figure, the magnetic

field results in a Lorentz force acting on the charge carriers that reduces the drift velocity in both regions giving a classical magnetoresistance.

Experimental procedure.—We measure the magnetotransport in single-crystal graphene synthesized by chemical vapor deposition on Pt foil [15,16]. The three CVD-grown samples 1, 2, and 3 were prepared at temperatures of 1000 °C, 950 °C, and 900 °C, and hydrogen mass flow rates of 700, 500, and 380 sccm, respectively. The synthesized graphene is then coated with poly(methyl methacrylate) (PMMA) resist with a spinning speed of 2000 rpm and then transferred to a 300 nm SiO_2 on Si substrate by electrolysis method [15]. Electron-beam lithography using PMMA resist is used to establish Cr/Au contacts via liftoff and again to define the graphene in a Hall-bar geometry of 40 μm long and 10 μm wide via oxygen plasma etching. All three devices have the same geometry.

As discussed in detail elsewhere [16], the differences between the Raman spectra of the three samples suggest the presence of nanocrystalline carbon impurities on the continuous crystalline graphene layer; sample 1 has the greatest concentration of impurities and sample 3 has the least. These impurities do not correlate with mobility, and so for the purposes of this work, the samples simply have varying amounts of disorder.

A constant current of 10 nA is applied in the four-probe measurement. Figure 2(a) shows the zero-field conductivity as a function of back-gate-induced carrier density n_0 for samples 1, 2, and 3. We observe the typical approximately linear dependence of conductivity as a function of carrier density [7], and from the data we can extract the charge-impurity limited mobility μ of the three samples as 8300 $cm^2/V\,s$, 8100 $cm^2/V\,s$, and 10 700 $cm^2/V\,s$ for samples 1, 2, and 3, respectively (see the Supplemental Material [17]). These values of mobility are among the highest for CVD-grown graphene transferred to SiO_2. Also shown in Fig. 2(a) are data from an exfoliated graphene sample [11], which has charge-impurity limited mobility μ of 18 200 $cm^2/V\,s$.

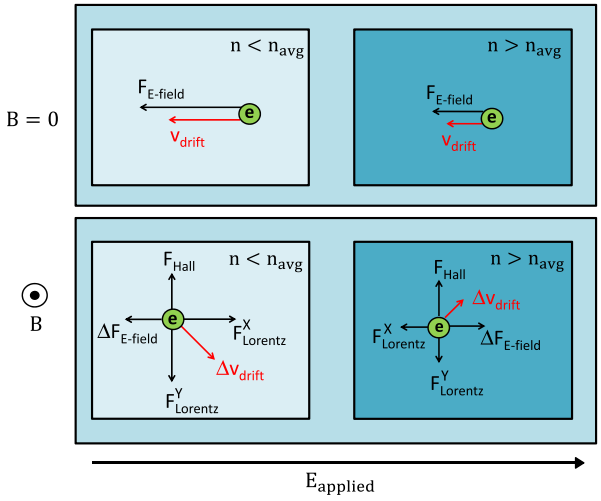

FIG. 1 (color online). In the upper panels, we show forces (apart from the drag force) and electron drift velocities in a sample with two regions of different charge carrier concentrations when there is no magnetic field. The bottom left (right) panel illustrates a region of higher (lower) carrier concentration than the sample average along with all the new forces that appear (apart from the change in drag force) when the magnetic field is applied. The change in drift velocity $\Delta v_{\rm drift}$ is against the direction of motion of the electron for both regions shown in the bottom panels and this is the microscopic origin of magnetoresistance.

We also experimentally measure the minimum conductivity $\sigma_{\rm min}$, and use this to extract the disorder-induced carrier density fluctuations $n_{\rm rms}$ using $\sigma_{\rm min} = n_{\rm rms} e\mu/\sqrt{3}$. The $\sqrt{3}$ factor comes from an effective medium theory calculation at zero magnetic field (see Ref. [18]). The values for $n_{\rm rms}$ extracted this way are between 20% and 40% lower than what one would expect from the self-consistent theory for graphene transport [19] that is normally [7] used to understand the graphene minimum conductivity. We attribute this discrepancy to the non-perfect transmission across p-n junctions separating the electron and hole regions or additional scattering by the nanocrystalline grain boundaries. As will become clearer later, we parametrize our data as a function of the ratio $n_0/n_{\rm rms}$, where both the average carrier density n_0 and the density fluctuations $n_{\rm rms}$ are measured independently.

Figure 2(b) shows the longitudinal resistance R_{xx} and Hall conductivity σ_{xy} as a function of back-gate voltage for all three samples at $T = 4.2$ K and $B = 8$ T. The data clearly show Subnikov–de Haas oscillations and quantum Hall plateaus with $\sigma_{xy} = 4(n + 1/2)e^2/h$ (where the factor $1/2$ is the fingerprint of the π Berry's phase in monolayer graphene) [20–22]. Figure 2(c) shows the magnetoresistance at 4.2 K. At high magnetic field and low carrier densities, we sometimes observe a linear magnetoresistance. However, for sufficiently low magnetic fields, we always observe a quadratic magnetoresistance, where for different values of carrier density n_0 and density fluctuation $n_{\rm rms}$, we can fit our data to

$$\rho_{xx}(B) = \rho_{xx}(B = 0)[1 + A(\mu B)^2] \qquad (1)$$

and extract the dimensionless coefficient $A[n_0, n_{\rm rms}]$ from our data. We can also fit the data over a larger range of B using the phenomenological formula of Ref. [11], $\rho_{xx}(B) = \rho_{xx}(0)\{1 - \alpha + [\alpha/\sqrt{1 + 2A(\mu B)^2/\alpha}]\}^{-1}$, where α is a fitting parameter. Notice that for $\mu B \ll 1$, this phenomenological expression gives the same value for A as Eq. (1). These fits are shown in Fig. 2. Since we are interested in the classical magnetoresistance, we exclude quantum interference by removing the lowest magnetic fields in the fitting (see the Supplemental Material [17]). We also found no significant temperature dependence of A

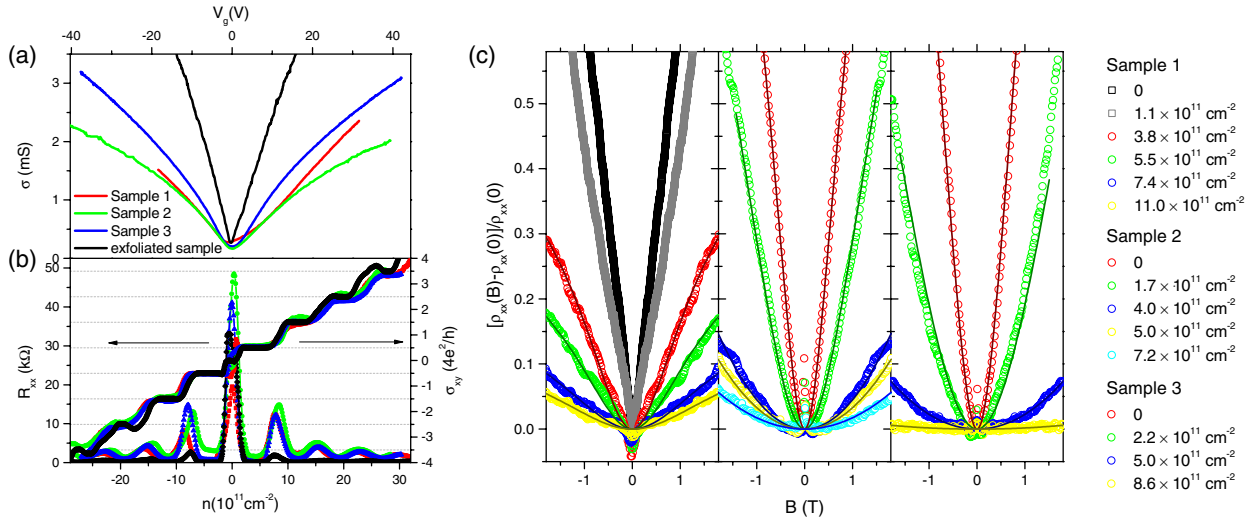

FIG. 2 (color online). Summary of the experimental results. (a) Conductivity as a function of carrier density n (back-gate voltage V_g) at zero magnetic field for CVD-grown samples 1, 2, and 3, and the exfoliated graphene sample from [11]. (b) Longitudinal resistance R_{xx} and Hall conductivity σ_{xy} as a function of carrier density n (back-gate voltage V_g) for CVD-grown samples 1, 2, and 3 and exfoliated sample at $T = 4.2$ K and $B = 8$ T. Top and bottom horizontal scales apply to both (a) and (b). (c) Low field magnetoresistance of samples 1 (left), 2 (middle), and 3 (right). Data are open symbols taken at the carrier density indicated in legend. Solid lines are fits described in the text.

between 4 and 50 K. Our main experimental observations in Fig. 3 are that $A[n_0, n_{\rm rms}]$ scales as a function of the ratio $n_0/n_{\rm rms}$ and that for large $n_0/n_{\rm rms}$ it follows a power law $A \sim (n_0/n_{\rm rms})^{-2}$ and persists far away from the Dirac point (i.e. $n_0 > n_{\rm rms}$) and is caused by carrier density inhomogeneity and not due to the presence of both electrons and holes close to the Dirac point.

Theoretical analysis.—The starting point for this analysis is to assume that the carrier density n is Gaussian distributed centered at an average carrier density n_0 with a rms fluctuation given by $n_{\rm rms}$ (we denote this distribution as $P[n, n_0, n_{\rm rms}]$). For the specific case of graphene, the authors of Ref. [18] justified theoretically the use of a Gaussian distribution, and at least close to charge neutrality, this has been seen in several experiments starting with Ref. [23]. In this context $\mathrm{sign}(n_0) = \pm 1$ represents the electron and hole bands, respectively. For the case where charged impurities dominate the transport properties, knowing the impurity concentration $n_{\rm imp}$ and the distance d away from the graphene sheet, one can calculate $n_{\rm rms}$ both analytically [19] (using the self-consistent approximation) and numerically [24] (using the mesoscopic density functional approach). The carrier mobility μ is calculated using the semiclassical Boltzmann transport theory [7]. In what follows, for simplicity, we assume that μ is density independent, and we show in the Supplemental Material [17] that the weak density dependence of the carrier mobility hardly changes any of our results. Since n_0 is controllably tuned by a back gate, and the parameters $n_{\rm imp}$ and d can be obtained from the conductivity at zero magnetic field, all the parameters used in our theory for magnetoresistance can be fixed by measurements done before applying a magnetic field.

Before discussing our inhomogeniety-induced magnetoresistance, we first briefly comment on previous theories for graphene magnetoresistance in the context of our framework. For a single channel model, it is easy to verify that there is no magnetoresistance i.e. $\rho_{xx}(B) = \rho_{xx}(0)$ [1]. The two-channel model [8] assumes that the total conductivity is the sum of the electron and hole channels, $\sigma_{xx} = \sigma^e_{xx} + \sigma^h_{xx}$, and similarly for the transverse conductivity, $\sigma_{xy} = \sigma^e_{xy} + \sigma^h_{xy}$. Defining $\eta = n_0/n_{\rm rms}$, a straightforward calculation gives the quadratic coefficient of the magnetoresistance (see definition above) as

$$A\left[\eta = \frac{n_0}{n_{\rm rms}}\right] = 1 - \left(\frac{\eta\sqrt{2\pi}}{2e^{-\eta^2/2} + \eta\sqrt{2\pi}\,\mathrm{Erf}(\eta/\sqrt{2})}\right)^2. \quad (2)$$

Here $\mathrm{Erf}(x)$ is the error function [25]. Notice that $A[\eta]$ is independent of the carrier mobility μ and depends only on the ratio of the carrier density and density fluctuation. This remains true so long as μ is independent of carrier density, and in this sense $A[\eta]$ becomes a universal function (where the different theoretical models each give a different functional form for $A[\eta]$). The two-channel result Eq. (2) is shown in Fig. 3; it has the value $A = 1$ at the Dirac point, stays roughly constant for $n_0 < n_{\rm rms}$, and then rapidly decreases for $n_0 > n_{\rm rms}$ as the second channel becomes depopulated. The inadequacy of this model to explain experimental data led the authors of Ref. [10] to develop an area-fraction effective medium theory. This model assumes that there are electron regions with area-fraction f_e and conductivity $\sigma_e = n_e e\mu$, and hole regions with f_h and $\sigma_h = n_h e\mu$. The effective medium conductivity tensor $\sigma_{\rm EMT}$ is obtained by solving $\sum_{i=e,h} f_i \delta\sigma_i (\mathbb{1}_2 - \Gamma\delta\sigma_i)^{-1} = 0$,

where the shorthand notation $\delta\sigma_i = \sigma_i - \sigma_{\rm EMT}$ is used. In the case where the electron and hole puddles can be assumed to be nearly circular, the depolarization tensor $\Gamma = -\mathbb{1}_2/(2\sigma^{xx}_{\rm EMT})$ takes a simple scalar form (see Ref. [26] for details). In this case, a remarkable result [9] is that when $n_0 = 0$ (and hence $f_e = f_h$), the magnetoresistance is given by $\rho_{xx}(B) = \rho_{xx}(0)\sqrt{1+(\mu B)^2}$. Since the self-consistent theory [19] gives $\rho_{xx}(0) = \sqrt{3}/(n_{\rm rms} e\mu)$ and $\mu[{\rm m}^2/{\rm V\,s}] \approx 50/(n_{\rm imp}[10^{10}\ {\rm cm}^{-2}])$, the full magnetoresistance at the Dirac point is completely specified. In particular, we have $A[0] = 1/2$. This model can be solved numerically away from the Dirac point, and the results are shown in Fig. 3. Notice again that for $n_0 > n_{\rm rms}$, the area fraction of the hole channel vanishes and the magnetoresistance drops rapidly.

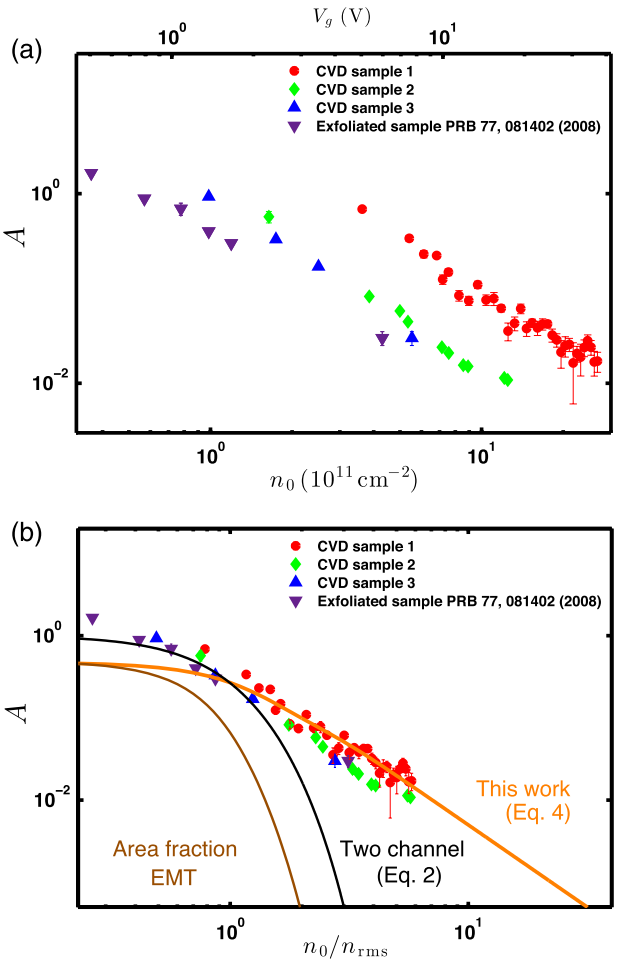

FIG. 3 (color online). Theoretical and experimental results for the dependence of the coefficient of quadratic magnetoresistance (a) plotted as a function of the carrier density n_0 and gate voltage V_g and (b) as a function of the ratio between carrier density n_0 and carrier density fluctuations $n_{\rm rms}$. The predictions of the earlier theoretical models including the two-channel model by Ref. [8] and the area fraction effective medium theory by Ref. [10] are shown as solid lines. In both earlier models, the magnetoresistance vanishes quickly once $n_0 > n_{\rm rms}$. By contrast, the magnetoresistance discussed in this work persists away from the Dirac point. For $n \gg n_{\rm rms}$, we find both theoretically and experimentally a power-law dependance: $A = (1/2)(n_0/n_{\rm rms})^{-2}$.

The inadequacy of the two-channel model is that it does not account for the spatial inhomogeneity of the carrier density, and the inadequacy of the area-fraction EMT is that although it allows for two-dimensional space to broken up into regions of electron and hole puddles, all electron and hole regions are assumed to be uniform. What is required is an effective medium approach with a continuous distribution of carrier density (similar to what has been developed in Refs. [27,28] for transport in zero-magnetic field). Using the form of the depolarization tensor derived in Ref. [26], for our system, we can derive a set of coupled equations

$$\int dnP[n,n_0,n_{\rm rms}]\frac{\sigma^2_{xx}[n]-(\sigma^{\rm EMT}_{xx})^2+(\sigma^{\rm EMT}_{xy}-\sigma_{xy}[n])^2}{(\sigma^{\rm EMT}_{xx}+\sigma_{xx}[n])^2+(\sigma^{\rm EMT}_{xy}-\sigma_{xy}[n])^2}=0, \tag{3a}$$

$$\int dnP[n,n_0,n_{\rm rms}]\frac{\sigma_{xy}[n]-\sigma^{\rm EMT}_{xy}}{(\sigma^{\rm EMT}_{xx}+\sigma_{xx}[n])^2+(\sigma^{\rm EMT}_{xy}-\sigma_{xy}[n])^2}=0. \tag{3b}$$

It is understood from Eq. (3) that $\sigma_{xx}[n]$ and $\sigma_{xy}[n]$ are obtained from some homogenous density model and then these coupled integral equations give the correct averaging over the density inhomogeneity. One can verify that for $B = 0$, we get $\sigma^{\rm EMT}_{xy} = 0$, and the equation for $\sigma^{\rm EMT}_{xx}$ reproduces the zero-magnetic field effective medium theory results of [18] and [27]. Moreover $\sigma^{\rm EMT}_{xy} = 0$ also for $n_0 = 0$, and a numerical solution of the $\sigma^{\rm EMT}_{xx}$ gives results very close to $\rho_{xx}(B) = \rho_{xx}(0)\sqrt{1+(\mu B)^2}$ (although, technically, it need not have given the same result since our model allows for carrier density inhomogeneity inside each puddle). We emphasize that Eq. (3) can be solved with any model for the density profile $P[n,n_0,n_{\rm rms}]$ and scattering potential as input for μ. In the simplified case where μ is independent of density, e.g. for charged impurity scattering, Eq. (3) simplifies considerably and the normalized magnetoresistance $\rho_{xx}(B)/\rho_{xx}(0)$ depends only on the ratios $n_0/n_{\rm rms}$ and μB. In this case, both $\sigma^{\rm EMT}_{xx}$ and $\sigma^{\rm EMT}_{xy}$ can be written in terms of dimensionless coefficients y_1 and y_2 as

$$\sigma^{\rm EMT}_{xx,xy} = y_{1,2} n_{\rm rms} e\mu/[1+(\mu B)^2], \tag{4}$$

where $y_{1,2} = y_{1,2}[n_0/n_{\rm rms}, \mu B]$ are computed in the Supplemental Material [17]. The coefficient of quadratic magnetoresistance obtained by solving these equations numerically has been plotted in Fig. 3.

It is important to notice that our inhomogeneous carrier density driven magnetoresistance persists far away from the Dirac point, and is not specific to the linear dispersion of graphene. Generally, there is remarkable agreement between the theoretical and experimental results presented

here. As we explain in the Supplemental Material [17], the discrepancy close to the Dirac point (for small values of n_0/n_{rms}) can be directly traced to the overestimation of σ_{min} in the self-consistent theory and corresponding difference between the theoretical and experimental values used for n_{rms} close to the Dirac point.

In summary we have shown both theoretical and experimental results for an inhomogeneity-induced quadratic magnetoresistance that scales as a power law of the ratio n_0/n_{rms}. While we focused on the case of charged impurities in graphene, the mechanism itself requires only spatial fluctuations in the carrier density and should therefore be observable in other systems.

The experimental work was supported by the University of Maryland NSF-MRSEC under Grant No. DMR 05-20471 and the U.S. ONR MURI program. M. S. F. acknowledges support from an ARC Laureate Fellowship. The theoretical work in Singapore was supported by the National Research Foundation Singapore under its fellowship program (NRF-NRFF2012-01).

*Current address: Department of Physics and Astronomy, University of Pennsylvania, 209 South 33rd Street, Philadelphia, PA 19104-6396, USA
†Current address: Department of Physics, Korea Advanced Institute of Science and Technology, Daejeon 305-701, Korea
‡shaffique.adam@yale-nus.edu.sg
§michael.fuhrer@monash.edu

[1] N. W. Ashcroft and N. D. Mermin, *Solid State Physics* (Holt, Rinehart, and Winston, New York, 1976).
[2] J. Nickel, Hewlett-Packard Laboratories Technical Reports **95–60**, 1 (1995).
[3] J. H. Ziman, in *Principles of the Theory of Solids* (Cambridge Academic Press, Cambridge, England, 1972).
[4] B. L. Altshuler, D. Khmel'nitzkii, A. I. Larkin, and P. A. Lee, Phys. Rev. B **22**, 5142 (1980).
[5] A. A. Abrikosov, Phys. Rev. B **58**, 2788 (1998).
[6] A. H. Castro Neto, F. Guinea, N. M. R. Peres, K. S. Novoselov, and A. K. Geim, Rev. Mod. Phys. **81**, 109 (2009).
[7] S. Das Sarma, S. Adam, E. H. Hwang, and E. Rossi, Rev. Mod. Phys. **83**, 407 (2011).
[8] E. H. Hwang, S. Adam, and S. Das Sarma, Phys. Rev. B **76**, 195421 (2007).
[9] V. Guttal and D. Stroud, Phys. Rev. B **71**, 201304 (2005).
[10] R. P. Tiwari and D. Stroud, Phys. Rev. B **79**, 165408 (2009).
[11] S. Cho and M. S. Fuhrer, Phys. Rev. B **77**, 081402 (2008).
[12] M. M. Parish and P. B. Littlewood, Nature (London) **426**, 162 (2003).
[13] M. M. Parish and P. B. Littlewood, Phys. Rev. B **72**, 094417 (2005).
[14] J. Hu, M. M. Parish, and T. F. Rosenbaum, Phys. Rev. B **75**, 214203 (2007).
[15] L. Gao *et al.*, Nat. Commun. **3**, 699 (2012).
[16] J. Ping and M. S. Fuhrer, arXiv:1304.5123 (J. Appl. Phys. (to be published)].
[17] See the Supplemental Material at http://link.aps.org/supplemental/10.1103/PhysRevLett.113.047206 for the insignificant temperature dependence of A, discussion of magnetoresistance for constant and nonconstant mobility near the Dirac point, and derivation of power-law scaling of $A[\eta]$.
[18] S. Adam, E. H. Hwang, E. Rossi, and S. Das Sarma, Solid State Commun. **149**, 1072 (2009).
[19] S. Adam, E. H. Hwang, V. M. Galitski, and S. Das Sarma, Proc. Natl. Acad. Sci. U.S.A. **104**, 18392 (2007).
[20] K. S. Novoselov, A. K. Geim, S. V. Morozov, D. Jiang, Y. Zhang, M. I. Katsnelson, I. V. Grigorieva, S. V. Dubonos, and A. A. Firsov, Nature (London) **438**, 197 (2005).
[21] Y. Zhang, Y.-W. Tan, H. L. Stormer, and P. Kim, Nature (London) **438**, 201 (2005).
[22] X. Wu, X. Li, Z. Song, C. Berger, and W. A. de Heer, Phys. Rev. Lett. **98**, 136801 (2007).
[23] J. Martin, N. Akerman, G. Ulbricht, T. Lohmann, J. H. Smet, K. von Klitzing, and A. Yacobi, Nat. Phys. **4**, 144 (2008).
[24] E. Rossi and S. Das Sarma, Phys. Rev. Lett. **101**, 166803 (2008).
[25] I. S. Gradshteyn and I. M. Ryzhik, *Table of Integrals, Series, and Products*, 5th ed. (Academic Press, New York, 1994).
[26] D. Stroud, Phys. Rev. B **12**, 3368 (1975).
[27] E. Rossi, S. Adam, and S. Das Sarma, Phys. Rev. B **79**, 245423 (2009).
[28] M. M. Fogler, Phys. Rev. Lett. **103**, 236801 (2009).